JACS
JOURNAL OF THE AMERICAN CHEMICAL SOCIETY

Communication

pubs.acs.org/JACS

Coronene-Containing N-Heteroarenes: 13 Rings in a Row

Alexander H. Endres,[†] Manuel Schaffroth,[‡] Fabian Paulus,[‡] Hilmar Reiss,[‡] Hubert Wadepohl,[†] Frank Rominger,[‡] Roland Krämer,[†] and Uwe H. F. Bunz*[,‡,§]

[†]Anorganisch-Chemisches and [‡]Organisch-Chemisches Institut, Ruprecht-Karls-Universität Heidelberg, Im Neuenheimer Feld 270, 69120 Heidelberg, Germany

[§]Centre for Advanced Materials, Ruprecht-Karls-Universät Heidelberg, Im Neuenheimer Feld 225, 69120 Heidelberg, Germany

Supporting Information

ABSTRACT: We describe the modular synthesis of three novel large N-heteroarenes, containing 9, 11, and 13 annulated rings. This modular system features fused azaacene units to a coronene nucleus. We evaluate the optical and electronic properties and the solid-state packing of the targets. The electronic properties of the 13-ring N-heteroarene allow the fabrication of a proof-of-concept thin-film transistor. Electron mobilities up to 8×10^{-4} cm/(V s) were obtained for polycrystalline films.

The privileged building blocks **7** and **8**–**10** build up a series of heteroarenes with 9, 11, or 13 linearly annulated six-membered rings, featuring a central coronene unit. The chemistry and evaluation of heteroarenes and heteroacenes have experienced a renaissance during the past decade.[1] Syntheses, structure, property evaluation, and uses in thin-film transistors demonstrate their potential.[2] Particularly interesting is the size of these ladder-oligomer-type species. For the pure N-heteroacenes, i.e., species that are composed entirely of catenated six-membered rings, azaheptacenes[3] are currently the largest persistent members, while in the case of N-heteroarenes both Mastalerz[4] and the group of Müllen[5] and others[6] have made strides towards extended heteroarenes; in these, azaacenes are sandwiched between aromatic units such as pyrene etc. that allow for more than one Clar-sextet. While such species are formally conjugated, they show band gaps that are increased in comparison to those of the azaacenes. The introduction of these building blocks increases stability and persistence.

The first reported extensions of the aromatic system of perylene diimides (PDIs) along the short molecular axis were achieved by a Diels–Alder reaction (bay-region of PDI) with maleic anhydride and simultaneous aromatization with chloranil.[7] Annulation in both bay-regions results in benzocoronene tetracarboxdiimide, first achieved by palladium-catalyzed dehydrohalogenation of 1,7-di(2-bromophenyl)-perylene diimide with DBU.[8] Today, an atom economic, phototriggered intramolecular cyclization accesses core-extended, functional coronenes from bay-substituted perylenes. Although this transformation has attracted considerable interest,[9] its regioselectivity has been less studied, rendering it difficult to predict its outcome. To avoid the inadvertent formation of zigzag constitutional compounds during the critical photocyclization step,[9e,10] we chose the symmetrical 2,3-dichloropyrazine **1** as our starting material, which was easily converted into the Stille-reagent **2** in 51% yield after deprotonation with LDA, followed by quenching with tributyltin chloride (Scheme 1).

Scheme 1. Synthesis of Coronene 7[a]

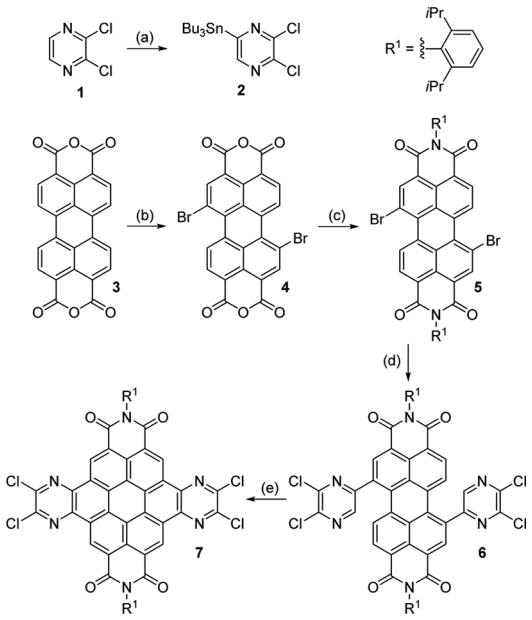

[a](a) LDA, Bu_3SnCl, THF, −100 °C, 51%; (b) Br_2, cat. I_2, H_2SO_4, 85 °C, 99%; (c) 2,6-diisopropylaniline, propionic acid, 140 °C, 81%; (d) **2**, $Pd(PPh_3)_4$, PhMe, 110 °C, 63%; (e) I_2, $h\nu$, rt, 87%.

This approach (Scheme 1) also ensured that the challenging separation of 1,6- and 1,7-regioisomeres,[11] usually formed during the bromination reaction of perylenetetracarboxylic acid dianhydride **3**, was unnecessary, since subsequent cyclization will give rise to the annulated product **7** regardless of the employed stereoisomer.

Synthesis of **7** proceeds along the established route from **3** to **5** via bromination of **3** to give **4** in 99% yield.[11a] Subsequent condensation with 2,6-diisopropyl-aniline afforded **5** in 81% yield.[12] Stille coupling of **2** and PDI **5** results in **6** (64%). We found that cyclization of **6** under irradiation by sunlight in refluxing toluene or DCM at room temperature was not

Received: December 3, 2015
Published: January 25, 2016

DOI: 10.1021/jacs.5b12642
J. Am. Chem. Soc. 2016, 138, 1792–1795

Scheme 2. Synthesis of Coronene-Containing N-Heteroarenes[a]

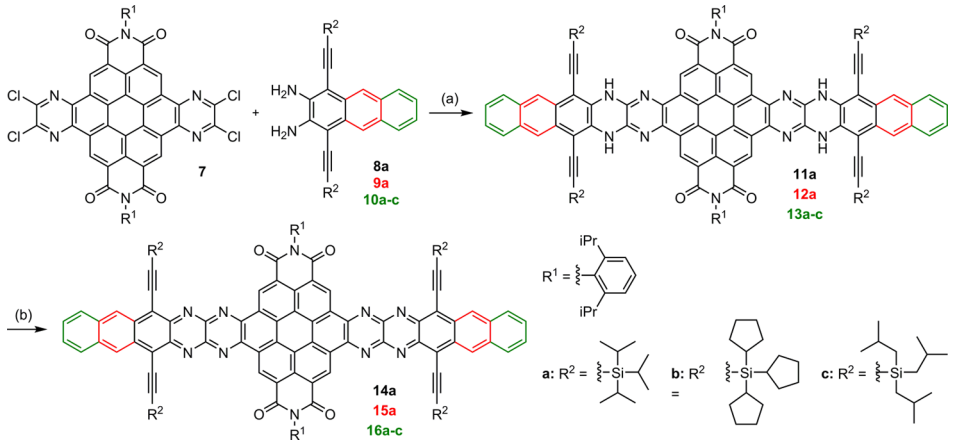

[a](a) Diamine (**8a**; **9a**; **10a–c**), $Pd(dba)_2$, RuPhos, DIPEA, $CHCl_3$, 60 °C, 83% (**11a**), 78% (**12a**), 72% (**13a**), 61% (**13b**), 67% (**13c**); (b) MnO_2, $CHCl_3$, rt, 79% (**14a**), 81% (**15a**), 73% (**16a**), 88% (**16b**), 91% (**16c**).

possible,[13] since only small amounts of product could be obtained.

Nonetheless, irradiation of a solution of **6** and catalytic amounts of iodine in chloroform with green light at room temperature resulted in 83% yield of **7**. **6** is soluble in most common organic solvents such as toluene, $CHCl_3$, THF, and acetonitrile, but **7** exhibits considerably lower solubility, due to increased π-stacking of the planar aromatic core. Similar systems with nitrogen-containing heterocoronene tetracarboxylic acid diimide analogues already display strong self-assembly into one-dimensional (1D) nanostructures in solution.[14]

The palladium-catalyzed coupling of *o*-diaminoarenes with *o*-dihaloarenes has been studied,[15] and a protocol for the coupling of diamines **8a–10c** with coronene derivative **7** was developed. DIPEA (Hünig's base) as sole solvent was not suitable, perhaps due to potential degradation of the diimide group on the perylene moiety. Due to the high reactivity of **7**, mixing with diamines **8a–10c**, [$Pd(dba)_2$], and RuPhos in chloroform and DIPEA as well as heating to 60 °C under argon was sufficient and resulted in satisfactory yields for **11a–13c** (61–83%, Scheme 2).

The *N*,*N*′-tetrahydrospecies **11a–13c** were oxidized with MnO_2 at room temperature. After removal of MnO_2, **14a–16c** were obtained by precipitation from the reaction mixture and purified by washing with acetonitrile, ethyl acetate, diethyl ether, and pentane. Column chromatography was unnecessary; **14a–16c** formed in yields above 73%. The oxidation process decreased the solubility of **14a–16c**, owing to increasing π-stacking. Therefore, the larger side groups tricyclopentylsilyl and tri-isobutylsilyl were introduced, since even saturated solutions of **16a** did not form proper thin films. Unexpectedly, **16b** exhibited an even lower solubility than **16a**, only halogenated arenes dissolve it. Only **16a** and **16c** exhibited a sufficient solubility for cyclic voltammetry and optical characterization.

In contrast to related annulated coronenes,[16] the tetrahydro compounds **11a–13a** feature a reversed order according to the lowest absorption band (Figure 1): The smallest **11a** shows a λ_{max} of 664 nm, in contrast to **12a** (650 nm) and **13a** (647 nm). However, the shift is small, indicating a minor impact of the attached acene moiety. Upon oxidation the strong, characteristic coronene-related bands undergo a substantial hypsochromic shift with the expected order of λ_{max}. Weak bands in the far red region develop with the longest wavelength at 1055 nm for **16a**.

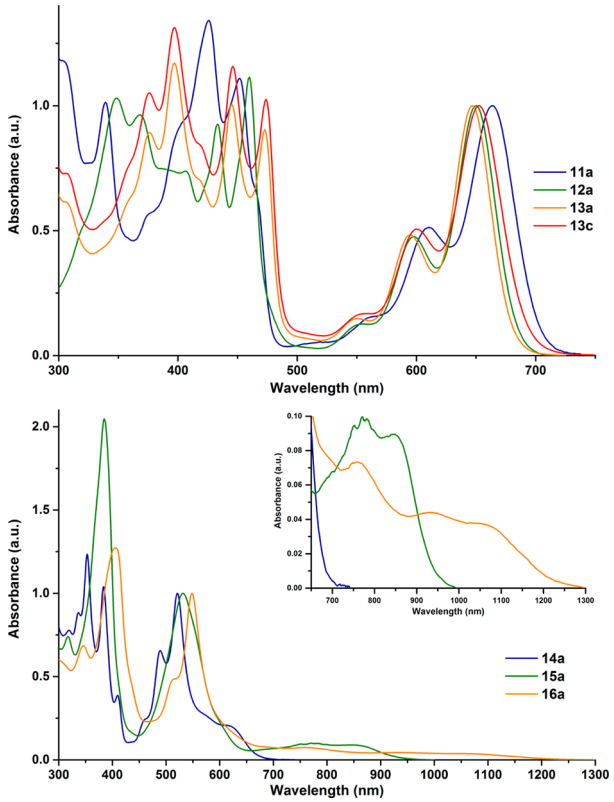

Figure 1. Absorption spectra of **11a–13c** (top) and **14a–16a** (bottom) in DCM solution.

Electronic properties of **14a–16c** were studied by cyclic voltammetry. For the larger systems **15a** and **16a,c**, four fully reversible reduction potentials were measured; for **14a** only two reversible reductions could be recorded due to solvent limitations (Figure 2, see SI for details). Measurements were performed in DCM with ferrocene/ferrocenium as internal standard and $(Bu_4N)^+(ClO_4)^-$ as electrolyte. First reduction potentials increased from −0.55 V to −0.41 V to −0.35 V going from **14a** to **16a**, which translates into LUMO energies of −4.25 eV, −4.39 eV, and −4.45 eV.[17]

DOI: 10.1021/jacs.5b12642
J. Am. Chem. Soc. 2016, 138, 1792–1795

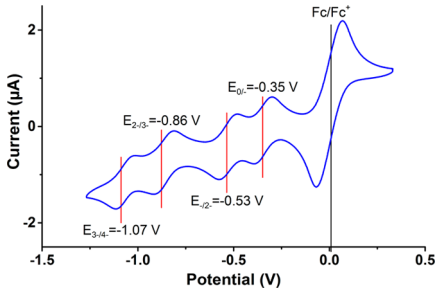

Figure 2. Cyclic voltammogram of **16a** shows four fully reversible reductions.

The optical gap of **14a**−**16c** was obtained from the onset of the lowest energy absorption band (Table 1). Subsequently, the HOMO energy was calculated as the difference of the LUMO energy from cyclic voltammetry and the optical gap. These experimental values are supported by DFT calculations (B3LYP/6-311G*). The calculated and experimental FMO energies are in good agreement (±0.2 eV). Despite the large π-systems, unrestricted calculations resulted in closed-shell singlet ground states.

The HOMO is mainly located on the aceneic parts of the molecule (Figure 3) because of the electron-deficient coronene core. In contrast, the LUMO is spread over the whole π-system. It features the largest coefficients at the coronene moiety, also as expected.

Another indication for the disturbance of the coronene core by the attached acene motive is provided by NICS scan calculations ($NICS(1)_{\pi zz}$, see SI for details).[18] For the tetrahydro species **13**, the different rings in the coronene core show similar diatropic ring currents, whereas, in the case of **16**, the ring directly attached to the acene part exhibits diminished NICS values of −12.2 ppm, and the center ring almost shows no current at all (see SI, Figure S55).

For the tri-isobutyl compound **16c**, a crystal structure was obtained (Figure 4). The π-system is fully planar, but slightly wavy. As expected, the silyl groups show a slight disorder and experience a distortion of 10° and 12° out of the plane of the π-system. The ring of the di-isopropylphenyl substituents at the bisimide moiety form an angle of 72° with the aromatic core.

The packing features 1D stacks with π−π contacts to only two translationally equivalent neighbors with a mean plane distance of 3.38 Å. The large spacial overlap of two molecules expands to the central ring of the coronene core and leads, in combination with the spread out LUMO distribution, to a large calculated LUMO−LUMO transfer integral of 125 meV and a calculated HOMO−HOMO transfer integral of 10.2 meV, (see SI for details),[19] making **16c** an attractive candidate for electron transport.

Crystal structures were also obtained from **13a** and **14a** (see SI for details). However, incorporated solvent molecules cloud information about the stacking properties; the molecular structure was confirmed nevertheless. Due to its promising

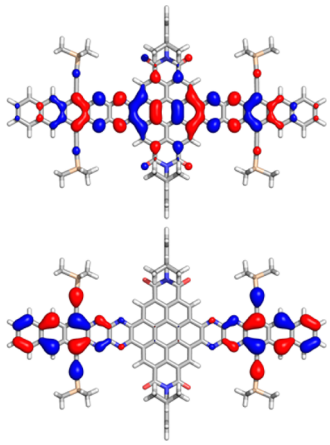

Figure 3. Calculated HOMO (top) and LUMO (bottom) distribution of **16** (for simplification, TMS side groups were used).

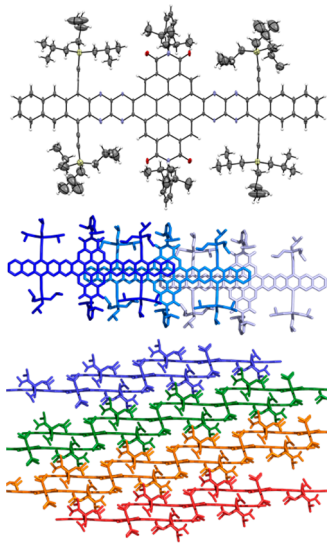

Figure 4. Top: Molecular structure of **16c** (50% probability plot). Middle: Top view of 1D stacks in crystal of **16c**. Bottom: Side view of the arrangement of neighboring stacks of **16c**.

electronic properties, the large transfer integral, and its high solubility, we evaluated the charge transport of **16c** in thin-film transistors.

The organic field-effect transistors were fabricated in bottom-contact/top-gate architecture (BC/TG) with gold source and drain electrodes (see SI). The active layer was deposited through spin-coating, resulting in polycrystalline films with domains of a few micrometres size (Figure 5a). Perfluorinated CYTOP-polymer was used as dielectric layer, and a thermally evaporated gate electrode finished the devices. These transistors display negligible hysteresis, a linear injection behavior, low threshold voltages (V_{th} = −(0.6 ± 1.2) V) and mediocre on/off ratios (>10^3) (see Figure 5b). As expected from the low LUMO

Table 1. Spectroscopic and Electrochemical Properties of Oxidized Heteroarenes 14a−16c

compd	$\lambda_{onset,abs}$ (nm)	Gap_{opt} (eV)	E_{red} (V)	$E_{LUMO,CV}$ (eV)	$E_{HOMO,opt}$ (eV)	$E_{HOMO,DFT}$ (eV)	$E_{LUMO,DFT}$ (eV)	Gap_{DFT} (eV)
14a	690	1.80	−0.55	−4.25	−6.05	−6.25	−4.27	1.98
15a	951	1.30	−0.41	−4.39	−5.69	−5.80	−4.33	1.46
16a	1300	0.95	−0.35	−4.45	−5.40	−5.46	−4.35	1.11
16c	1199	1.03	−0.37	−4.43	−5.46	−5.46	−4.35	1.11

DOI: 10.1021/jacs.5b12642
J. Am. Chem. Soc. 2016, 138, 1792−1795

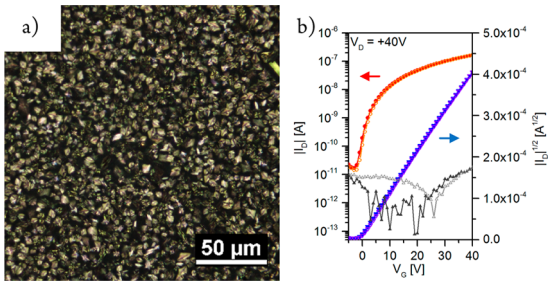

Figure 5. (a) Image of a polycrystalline film of **16c** under crossed polarizers. (b) Transfer characteristic of **16c** in a BC/TG FET (W = 1000 μm, L = 10 μm) at V_D = 40 V; gate leakage in the background; filled symbols, forward; open symbols, backward sweep.

energy, **16c** transports electrons with an average saturation mobility of $\mu_e = (3.9 \pm 2.4, \text{best device } 8.1) \times 10^{-4}$ cm^2/(V s); at higher drain voltages ambipolar transport was observed ($\mu_h \approx 2 \times 10^{-4}$ cm^2/(V s), see SI).

The relatively low charge carrier mobility is attributed to the small domain size and polycrystalline nature of the fabricated films of **16c**. Further optimization, to increase the domain size and boost charge carrier mobility of **16c**, is currently under investigation.

In conclusion, we demonstrate synthesis and comprehensive analysis of a series of stable and soluble extended heterocyclic π-systems. Easily accessible coronene **7** serves as a privileged building block accessing coronene incorporated N-heteroarenes **14a**−**16c**. The initial results highlight their potential as a new class of materials for organic electronic devices. The symmetrical and rigid nature of **7** suggests applications as building block in ladder-type polymers and molecular wires. Extended structures like **16** show the limits for valuable conjugated small molecules; increasing π-stacking demands larger solubilizing groups preventing tight molecular packing. With that in mind, considerably larger, well-defined ladder-type N-heteroarenes should be accessible.

■ ASSOCIATED CONTENT

Supporting Information

The Supporting Information is available free of charge on the ACS Publications website at DOI: 10.1021/jacs.5b12642.

Experimental and spectroscopic data (PDF)
Crystallographic data (CIF)
Crystallographic data (CIF)

■ AUTHOR INFORMATION

Corresponding Author

*uwe.bunz@oci.uni-heidelberg.de

Notes

The authors declare no competing financial interest.

■ ACKNOWLEDGMENTS

M.S. and U.H.F.B. thank the Deutsche Forschungsgemeinschaft (DFG Bu771/7-2).

■ REFERENCES

(1) (a) Bunz, U. H. F.; Engelhart, J. U.; Lindner, B. D.; Schaffroth, M. *Angew. Chem., Int. Ed.* **2013**, *52*, 3810−3821. (b) Bunz, U. H. F. *Pure Appl. Chem.* **2010**, *82*, 953−968. (c) Bunz, U. H. F. *Acc. Chem. Res.* **2015**, *48*, 1676−1686. (d) Li, J.; Zhang, Q. *ACS Appl. Mater. Interfaces* **2015**, *7*, 28049−28062. (e) Miao, Q. *Synlett* **2012**, *23*, 326−336.
(2) Miao, Q. *Adv. Mater.* **2014**, *26*, 5541−5549.
(3) Engelhart, J. U.; Tverskoy, O.; Bunz, U. H. F. *J. Am. Chem. Soc.* **2014**, *136*, 15166−15169.
(4) Kohl, B.; Rominger, F.; Mastalerz, M. *Angew. Chem., Int. Ed.* **2015**, *54*, 6051−6056.
(5) Fogel, Y.; Kastler, M.; Wang, Z.; Andrienko, D.; Bodwell, G. J.; Müllen, K. *J. Am. Chem. Soc.* **2007**, *129*, 11743−11749.
(6) (a) Wang, C.; Zhang, J.; Long, G.; Aratani, N.; Yamada, H.; Zhao, Y.; Zhang, Q. *Angew. Chem., Int. Ed.* **2015**, *54*, 6292−6296. (b) More, S.; Choudhary, S.; Higelin, A.; Krossing, I.; Melle-Francoe, M.; Mateo-Alonso, A. *Chem. Commun.* **2014**, *50*, 1976−1979. (c) Kotwica, K.; Bujak, P.; Wamil, D.; Materna, M.; Skorka, L.; Gunka, P. A.; Nowakowski, R.; Golec, B.; Luszczynska, B.; Zagorska, M.; Pron, A. *Chem. Commun.* **2014**, *50*, 11543−11546. (d) Takeda, Y.; Okazaki, M.; Minakata, S. *Chem. Commun.* **2014**, *50*, 10291−10294. (e) Gao, B.; Wang, M.; Cheng, Y.; Wang, L.; Jing, X.; Wang, F. *J. Am. Chem. Soc.* **2008**, *130*, 8297−8306.
(7) Langhals, H.; Kirner, S. *Eur. J. Org. Chem.* **2000**, *2000*, 365−380.
(8) Müller, S.; Müllen, K. *Chem. Commun.* **2005**, 4045−4046.
(9) (a) Zhong, Y.; Kumar, B.; Oh, S.; Trinh, M. T.; Wu, Y.; Elbert, K.; Li, P.; Zhu, X.; Xiao, S.; Ng, F.; Steigerwald, M. L.; Nuckolls, C. *J. Am. Chem. Soc.* **2014**, *136*, 8122−8130. (b) Zhang, Y.; Chen, L.; Zhang, K.; Wang, H.; Xiao, Y. *Chem. - Eur. J.* **2014**, *20*, 10170−10178. (c) Zhao, Z.; Zhang, Y.; Xiao, Y. *J. Org. Chem.* **2013**, *78*, 5544−5549. (d) Xie, Y.; Zhang, X.; Xiao, Y.; Zhang, Y.; Zhou, F.; Qi, J.; Qu, J. *Chem. Commun.* **2012**, *48*, 4338−4340. (e) Li, Y.; Xu, L.; Liu, T.; Yu, Y.; Liu, H.; Li, Y.; Zhu, D. *Org. Lett.* **2011**, *13*, 5692−5695. (f) Müller, M.; Mauermann-Düll, H.; Wagner, M.; Enkelmann, V.; Müllen, K. *Angew. Chem., Int. Ed. Engl.* **1995**, *34*, 1583−1586.
(10) Müller, U.; Enkelmann, V.; Adam, M.; Müllen, K. *Chem. Ber.* **1993**, *126*, 1217−1225.
(11) (a) Würthner, F.; Stepanenko, V.; Chen, Z.; Saha-Möller, C. R.; Kocher, N.; Stalke, D. *J. Org. Chem.* **2004**, *69*, 7933. (b) Ma, J.; Yin, L.; Zou, G.; Zhang, Q. *Eur. J. Org. Chem.* **2015**, *2015*, 3296−3302.
(12) Kohl, C.; Weil, T.; Qu, J.; Müllen, K. *Chem. - Eur. J.* **2004**, *10*, 5297−5310.
(13) Yuan, Z.; Xiao, Y.; Qian, X. *Chem. Commun.* **2010**, *46*, 2772−2774.
(14) Li, Y.; Li, Y.; Li, J.; Li, C.; Liu, X.; Yuan, M.; Liu, H.; Wang, S. *Chem. - Eur. J.* **2006**, *12*, 8378−8385.
(15) (a) Engelhart, J. U.; Lindner, B. D.; Tverskoy, O.; Rominger, F.; Bunz, U. H. F. *Chem. - Eur. J.* **2013**, *19*, 15089−15092. (b) Lindner, B. D.; Engelhart, J. U.; Tverskoy, O.; Appleton, A. L.; Rominger, F.; Peters, A.; Himmel, H.-J.; Bunz, U. H. F. *Angew. Chem., Int. Ed.* **2011**, *50*, 8588−8591. (c) Tverskoy, O.; Rominger, F.; Peters, A.; Himmel, H.-J.; Bunz, U. H. F. *Angew. Chem., Int. Ed.* **2011**, *50*, 3557−3560. (d) Biegger, P.; Stolz, S.; Intorp, S. N.; Zhang, Y.; Engelhart, J. U.; Rominger, F.; Hardcastle, K. I.; Lemmer, U.; Qian, X.; Hamburger, M.; Bunz, U. H. F. *J. Org. Chem.* **2015**, *80*, 582−589.
(16) Lütke Eversloh, C.; Li, C.; Müllen, K. *Org. Lett.* **2011**, *13*, 4148−4150.
(17) Cardona, C. M.; Li, W.; Kaifer, A. E.; Stockdale, D.; Bazan, G. C. *Adv. Mater.* **2011**, *23*, 2367−2371.
(18) (a) Rahalkar, A.; Stanger, A. *Aroma*, http://tx.technion.ac.il/~stanger/aroma/. (b) Stanger, A. *J. Org. Chem.* **2006**, *71*, 883−893. (c) Stanger, A. *J. Org. Chem.* **2010**, *75*, 2281−2288. (d) Gershoni-Poranne, R.; Stanger, A. *Chem. - Eur. J.* **2014**, *20*, 5673−5688.
(19) (a) Kirkpatrick, J. *Int. J. Quantum Chem.* **2008**, *108*, 51−56. (b) Baumeier, B.; Kirkpatrick, J.; Andrienko, D. *Phys. Chem. Chem. Phys.* **2010**, *12*, 11103−11113.

DOI: 10.1021/jacs.5b12642
J. Am. Chem. Soc. 2016, 138, 1792−1795